

## RECENT ADVANCES IN SMART-MATERIAL ROTOR CONTROL ACTUATION.

Victor Giurgiutiu\*,

University of South Carolina, Mechanical Engineering Department, Columbia, SC 29208

### ABSTRACT

This paper reviews recent achievements in the application of active-materials actuation to counteract aeroelastic and vibration effects in helicopters and fixed wing aircraft. A brief review of the induced-strain actuation principles and capabilities is done first. Attention is focused on the smart rotor-blade applications. The induced twist, active blade tip, and active blade flap concepts are presented and discussed. A number of ingenious displacement amplifications methods, both solid-state and levered, are described. Emphasis is placed on experimental results that prove the expectations and reveal the possible limitations of each particular concept. Full-scale smart rotor efforts are also highlighted. Conclusions and directions for further work are presented

### INTRODUCTION

Aeroelastic and vibration control technology allows flight vehicles to operate outside the traditional flutter limitations, improves ride qualities, and minimizes vibration fatigue damage. Conventional active flutter and vibration control technology relies on the use of aerodynamic control surfaces operated by servo-hydraulic actuators. In this conventional configuration, the flutter and vibration suppression algorithms are implemented through the servo-valve/hydraulic actuator. Though widely used, conventional technologies for active control of flutter and vibrations have severe limitations (Giurgiutiu, 1995) such as: (a) multiple energy conversions (mechanical, hydraulic, electrical); (b) large number of parts, i.e., potential failure sites; (c) high vulnerability of the hydraulic pipes network. In contrast, active-materials technologies offers direct conversion of electrical energy to high-frequency linear motion.

\*Associate Professor, Member AIAA, AHS, ASME, ASCE, RAeS

### BACKGROUND

#### Active-Materials Induced Strain Actuation

Active materials exhibit induced-strain under the action of an electric or magnetic field. Most common active materials are:

- a) PZT - Lead Zirconate Titanate —a ferroelectric ceramic material with piezoelectric properties and reciprocal behavior that converts electrical energy into mechanical energy and vice-versa. PZT-5 is one of the most widely used formulations for actuator applications. The behavior of the PZT material is quasi-linear, though hysteretic. Reversed polarity can be accommodated in moderate quantities (25-30%).
- b) PMN - Lead Magnesium Niobate — An electrostrictive ceramic material with piezoelectric properties. PMN does not accept reverse polarity, but has much less hysteresis.
- c) TERFENOL - TER (Terbium) FE (Iron) NOL (Naval Ordnance Laboratory) — a magnetostrictive alloy consisting primarily of Terbium, Dysprosium, and Iron. In practice, TERFENOL materials are made to exhibit quasi-linear piezomagnetic behavior through the application of bias fields.

Commercially available high-performance induced-strain actuators (piezo-electric, electro-strictive, or magneto-strictive) are capable of large forces and up to 0.1% strain (Figure 1a). This creates the opportunity for direct electrical-to-mechanical energy conversion. Electrical energy is easier to transmit throughout the aircraft, and electric lines are much less vulnerable than hydraulic pipes. The implementation of active-materials induced-strain actuation eliminates the need for hydraulic power systems, and relies directly on electrical-to-mechanical conversion (Figure 1b). In spite of large force and energy capabilities, active-materials induced-strain actuators (ISA) have very small strokes, limited by the inherent 0.1% cap on the induced strain response (Giurgiutiu *et al.*, 1996, 1997b). For example, a 100-mm long actuator is capable of a mere 0.1-mm peak-to-peak stroke. Practical implementation of induced

strain actuators into aircraft control system must include displacement amplification mechanisms (Giurgiutiu *et al.*, 1997a).

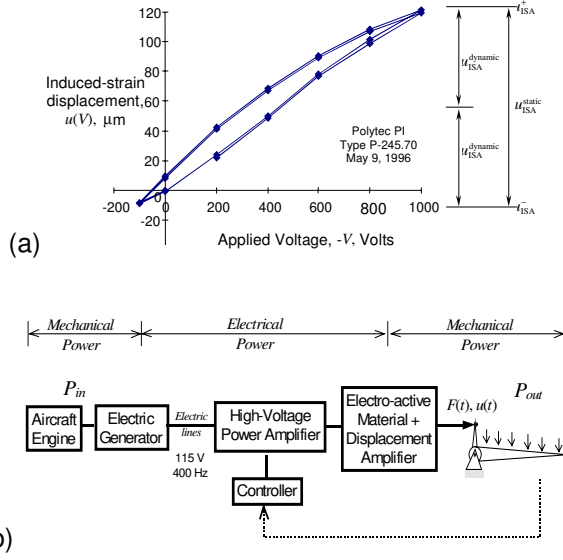


**Figure 1 Active materials offer direct conversion of electrical energy in high frequency linear motion. However, their implementation into aircraft hydraulic system cannot be achieved without displacement amplification.**

The modeling of active materials behavior is achieved, in the first approximation, through the general constitutive equations of linear piezoelectricity (ANSI/IEEE Standard 176-1987) which describe a tensorial relation between mechanical and electrical variables (mechanical strain  $S_{ij}$ , mechanical stress  $T_{ij}$ , electrical field  $E_i$ , and electrical displacement  $D_i$  in the form:

$$\begin{aligned} S_{ij} &= s_{ijkl}^E T_{kl} + d_{kij} E_k \\ D_j &= d_{jkl} T_{kl} + \epsilon_{jk}^T E_k, \end{aligned} \quad (1)$$

where  $s_{ijkl}^E$  is the mechanical compliance of the material measured at zero electric field ( $E = 0$ ),  $\epsilon_{jk}^T$  is the dielectric permittivity measured at zero mechanical stress ( $T = 0$ ), and  $d_{kij}$  is the piezoelectric coupling between the electrical and mechanical variables. For magneto-active materials, a set of equations similar to Equations (1) can also be derived:

$$\begin{aligned} S_{ij} &= s_{ijkl}^E T_{kl} + d_{kij} H_k \\ D_j &= d_{jkl} T_{kl} + \mu_{jk}^T H_k \end{aligned} \quad (2)$$

where,  $H_k$  is the magnetic field intensity, and  $\mu_{jk}^T$  is the magnetic permeability under constant stress. The coefficients  $d_{kij}$  are now defined in terms of magnetic units. The magnetic field intensity  $H$  in a rod of length  $L$  is related to the current in the surrounding coil (with  $n$  turns per unit length) through the expression:

$$H = nI \quad (3)$$

### **Power, Energy, and Efficiency of Active-Materials Induced-Strain Actuation**

Due to the small induced-strain capability of currently available active materials (typically, 0.1%), the active material actuators must necessarily include a displacement amplification scheme. Therefore, the power, energy, and efficiency of active-materials induced-strain actuation depend on two major factors: (a) active-material intrinsic properties; and (b) design characteristics of the active materials embedment and displacement amplification scheme. Giurgiutiu *et al.* (1996, 1997b) studied the intrinsic properties of commercially available active-material transducers. Full stroke conditions were considered, and a secant linearization approach was adopted. The maximum energy output from the induced-strain actuator was calculated for the matched stiffness conditions, i.e., when the internal stiffness of the actuator equals the stiffness of the external application. Typical energy density values found in these studies were placed in the range, 2.71-15.05 J/dm<sup>3</sup> (0.292-1.929 J/kg) under static conditions, and 0.68-3.76 J/dm<sup>3</sup>, (0.073-0.482 J/kg) under dynamic conditions. Power densities of up to 23.6 kW/dm<sup>3</sup> (3.0 kW/kg) were predicted at 1 kHz. The overall efficiency of active-material actuation depends, to a great extend, on the efficiency of the entire system that includes not only the active-material transducer, but also the displacement amplification and the power supply.

### **Helicopter Applications**

Helicopter applications of induced-strain actuation has received extensive attention (Giurgiutiu *et al.*, 1994; Narkiewicz and Done, 1994; Chopra 1997). Conventional actuation solutions (hydraulics and electric motors) are impractical for on-blade actuation. Induced-strain appears as the only viable alternative. Two directions have been investigated: (a) distributed induced-strain actuation resulting in a continuous twisting of the blade; and (b) discrete actuation of a servo-

aerodynamic control surface (flap, tab, blade-tip, etc.) to generate localized aerodynamic forces.

### INDUCED BLADE TWIST

By distributing active material elements along the flight structure, a smooth continuous deformation is obtained. Since the active materials can be embedded in the structure, this solution has clear aerodynamic advantages over the discrete actuation concepts. A number of theoretical studies have been performed to estimate the degree of twist required to effect flutter and vibration reduction benefits (Nitzsche, 1993, 1994; Walz, and Chopra, 1994). These studies have been followed by extensive experimental work, as described next.

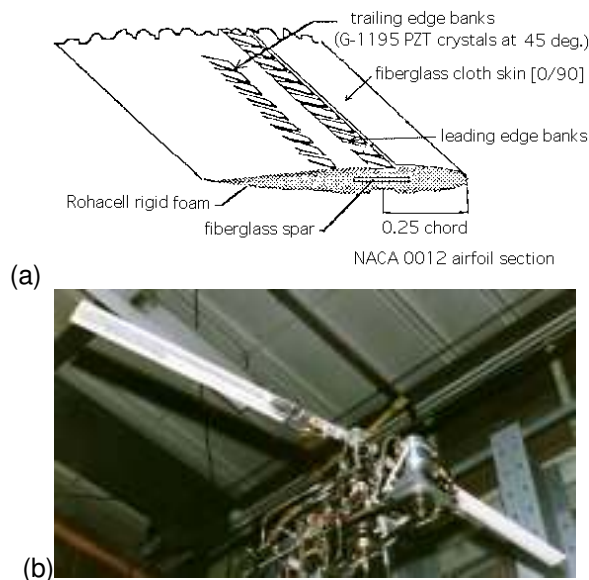


**Figure 2 Induced twist through diagonally embedded PZT crystals banks: (a) schematic of the arrangement (Chen and Chopra, 1997); (b) wind tunnel testing (Chopra, 1994).**

### Induced Twist through PZT Wafers Embedded in Composite Blade Structure

Chen and Chopra (1997) describe the construction of a 1/8-Froude scale composite blade with diagonally oriented PZT wafers embedded in the fiberglass skin (Figure 2). Electrical activation of the PZT wafers induces twist of the blade. The blade was tested in Glenn L. Martin Wind Tunnel at the University of Maryland. Dynamic tests were performed in non-rotating and rotating conditions. Significant twist response was measured when excitation was close to resonance frequencies (50 Hz and 95 Hz). Maximum tip twist values at resonance frequencies were  $0.35^\circ$  and  $1.1^\circ$ ,

respectively. At non-resonance frequencies, the response was very small (Chen and Chopra, 1997).

### Torque Plate Piezoelectric Actuator for Solid State Adaptive Rotors

Barrett (1993) build an electrically active torque plate consisting of a metallic substrate and diagonally attached PZT wafers. Twisting of the torque plate is created by activation of the PZT elements are with polarities on the top and bottom surfaces in opposing phase. A Solid State Adaptive Rotor (SSAR), consisting of the ISA torque plate attached to the root of a Froude scale composite blade, was constructed. Activation of the torque plates produce pitch deflections of the blade.

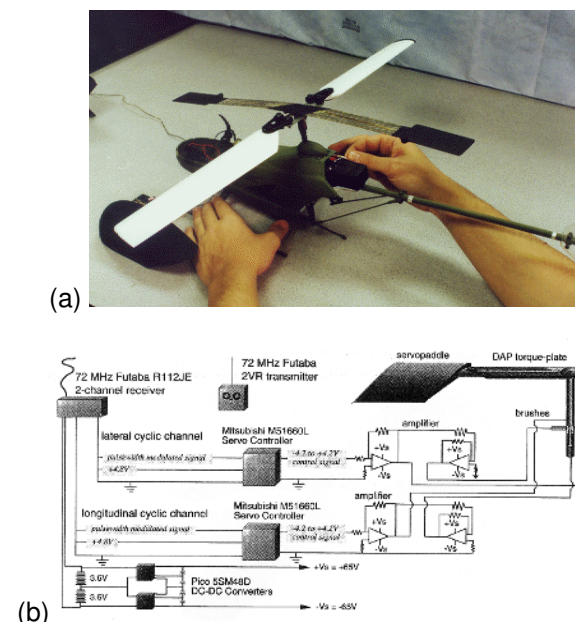


**Figure 3 Model helicopter Gamara, equipped with piezoelectrically activated Hiller paddle: (a) bench tests; (b) flight demonstration; (c) schematic of the power and active control systems (Barrett, Frye, and Schliesman, 1998)**

Bench tests showed a resonance peak at  $\sim 42$  Hz, followed by the typical 3 dB tail drop (Barrett and Stutts, 1997). The twist amplitude measured at resonance was in excess of  $10^\circ$ . The torque plate concept was applied to produce in-flight demonstration of a Kyosho Hyperfly helicopter model, featuring a Hiller servo-paddles control system was used. The complicated swash-plate assembly was stripped from the model helicopter and full control authority was turned over to a pair of ISA-activated Hiller servo-paddles (Figure 3). Removal of the swash-plate assembly reduced the flight controls weight by 40%, the aircraft gross

weight by 8%, and the parasite drag by 26% through appropriate fairing (Barrett, Frye, and Schliesman, 1998). Flight testing of the model was successfully performed.

### **Active Fiber Composites for Rotor Blade Twist**

Active fiber composites (AFC) consist of a laminated structure of fiberglass plies and PZT-fiber plies. The PZT-fiber plies have continuous, aligned, PZT fibers in an epoxy layer, and polyimide/copper electrode films (Figure 4). The electrode films are etched into an inter-digitated pattern that effects electric field along the fiber direction, thus activating the primary  $d_{33}$  piezoelectric effect (Rodgers and Hagood, 1998).

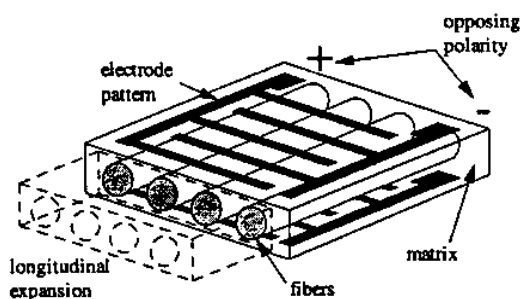
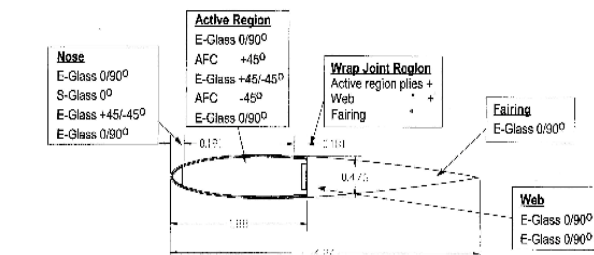
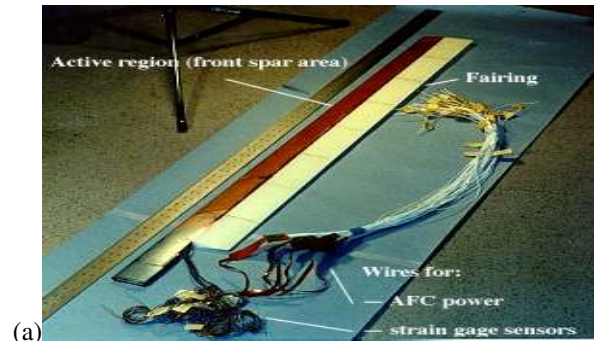


**Figure 4 Schematic representation of PZT-fiber composite illustrating the inter-digitated electrodes and the longitudinal expansion of the fibers (Rodgers and Hagood, 1998).**

In one project (Rodgers and Hagood, 1998), active fiber composite was incorporated into the construction of a 1/6<sup>th</sup> Mach scale CH-47D blade model (60.619-in span and 5.388-in chord) for wind tunnel testing at Boeing Helicopters, PA. Three diagonally placed AFC plies were incorporated in the co-cured D-spar blade lay-up. Activation of the diagonally placed fibers induces shear in the spar skin, which generates blade twist. A design goal of  $\pm 2^\circ$  blade twist was set. The blade specimen contained 7 groups of 6 AFC packs (3 in the top plies and 3 in the bottom). Of the 42 AFC packs installed in the blade, 11 were found to have poor electrical connection, and could not be activated. Thus, the blade actuation authority was somehow impaired. Bench tests performed at frequencies up to 67.5 Hz demonstrated a maximum twist authority of between 1 and 1.5° peak-to-peak ( $\pm 0.5 - 0.75^\circ$  amplitude). The full-length blade specimen was tested in a hover stand at 800 to 1336 rpm. The blade demonstrated hover testing resulted in recorded torsional strain and vertical hub force. At present, the active fiber technology is undergoing

environmental stress evaluation (Morris, Pizzochero, and Hagood, 1999).



(b)



(c)

**Figure 5 Active Twist Rotor (ATR): (a) Final ATR prototype blade; (b) AFC placement in the active blade; (c) ATR mounted in the Transonic Dynamic Tunnel (TDT) at NASA Langley Research Center (Cesnik, 1999).**

In a separate project, AFC plies were incorporated into an NASA/ARL/MIT active twist rotor (ATR) blade tested in the Transonic Dynamic Tunnel (TDT) at NASA Langley Research Center (Figure 5). The tunnel was filled with heavy gas (2.4 kg/m<sup>3</sup>) to achieve Mach-scale similarity. Based on measure bending moment response, it was estimated that 1 to 1.5 deg. maximum twist was generated for the  $4 \pm 1/\text{rev}$  (33--55 Hz) frequency range at 1000 V electric excitation (Wilbur *et al.* (1999). Simulated forward flight experiments of an improved rotor are being scheduled. Aeroelastic modeling of the ATR performance was performed by Wilkie *et al.* (1999). Extensive modeling of the ATR blade actuation mechanism was performed by Cesnik *et al.* (1999), Cesnik and Shin (1999). A



two-cell model of the blade cross-section was developed, and stiffness parameter studies were performed to identify optimal configuration.

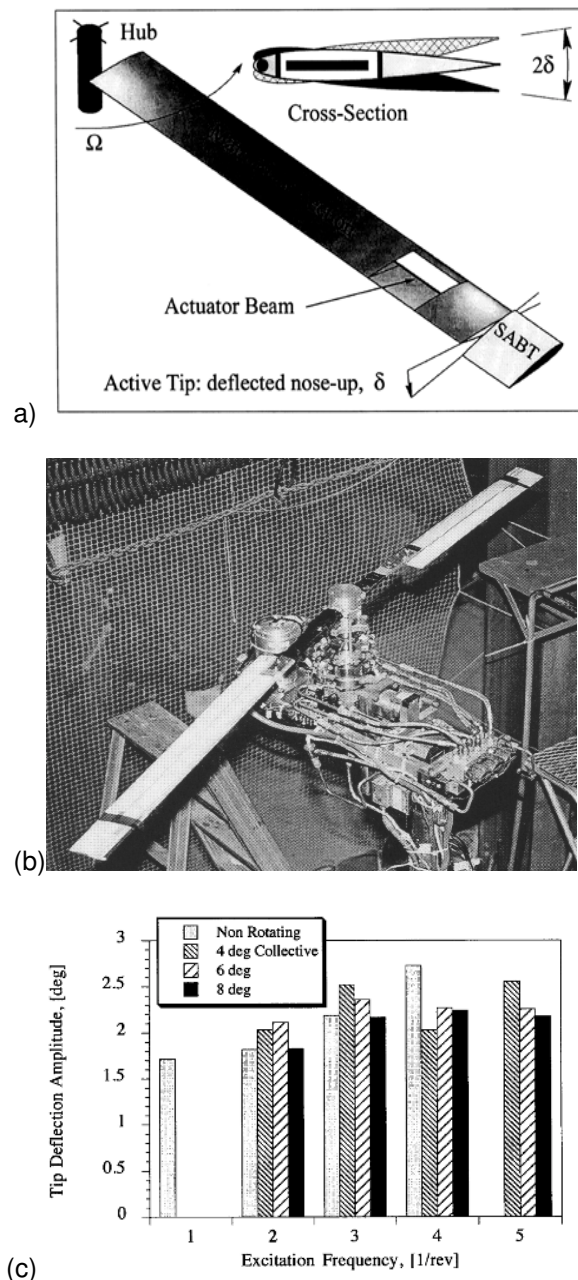


**Figure 6** Smart active blade tip (SABT): (a) the all-movable blade tip is driven by a span-long actuator beam placed inside the blade (b) SBAT 1/8<sup>th</sup> Froude scale model in the University of Maryland hover stand; (c) tip deflection up to 2.5° were recorded at 930 rpm (Bernhard and Chopra, 1999).

### Active Blade Tip with Bending-Torsion ISA Actuator

Bernhard and Chopra (1999) studied the Smart Active Blade Tip (SABT) concept for rotor blade vibrations and aeroelastic control (Figure 6a).

An all-movable blade tip is driven in rotational motion by a coupled bending-torsion induced-strain rotary-actuator placed inside the blade. The actuator consists of span-wise segments of structural layers [+45°/0°/-45°] and diagonally placed directionally attached PZT wafer actuators. The span-wise segments are differentially energized such that, the induced-strain bending curvatures cancel out, while the induced-strain twist curvatures add up to create a net tip rotation. A model-scale bending-torsion actuator beam (546 mm x 25.4 mm x 2 mm) was constructed and tested into a 6-ft (1.83 m) bearingless rotor model (1/8 Froude scale) with a 10% span movable tip. The blade tip response at 930 rpm varied between 2° and 2.5° for 1, 2, 3, 4, and 5/rev excitation frequencies (Figure 8c). Active blade twist experiments were also performed. Hover tests at 875 rpm produced blade twist results from 0.3° at 1/rev through 0.5° at 5/rev excitation.

### ROTOR BLADE FLAP ACTUATION

Servo-flap concepts have been investigated as a quicker-to-the-target approach to achieving induced-strain rotor blade actuation. Theoretical studies (Millott and Friedmann, 1994) highlighted the aerodynamic servo-flap concept benefits for active helicopter rotor control. The studies used an extensive aeroelastic model (including geometrical non-linearities and advanced unsteady aerodynamic 2-D models) that was coupled with a vibration-reduction controller. Substantial vibration reductions were demonstrated at various helicopter airspeeds corresponding to advance ratios in the range  $\mu = 0.0 - 0.4$ . The required flap travel, hinge moment, and average power consumption were calculated.

### Bimorph Servo-Flap Actuation

Bimorph piezoelectric actuators (Figure 7) were used in early servo-flap experiments targeting the Boeing CH-47D tandem helicopter (Spangler and Hall, 1989). A 1/5-scale stationary-model with a 10% chord flap was wind tunnel tested at various airspeeds between zero and 78 ft/sec, and at frequencies up to 100 Hz. Significant flap deflection, lift, and pitching moments were recorded, but the values were significantly below the theoretical predictions.

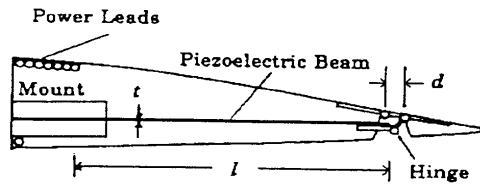


**Figure 7 Early bimorph-activated trailing-edge flap specimen (Sprangler and Hall, 1989).**

An improved design using a multilayer ISA bender actuator, solid-state flexural hinges, and impedance matching principles, was subsequently conceptualized, manufactured, and tested (Hall and Precht, 1996), with good bench test results ( $\pm 11^\circ$  flap deflection over 0-90 Hz bandwidth).

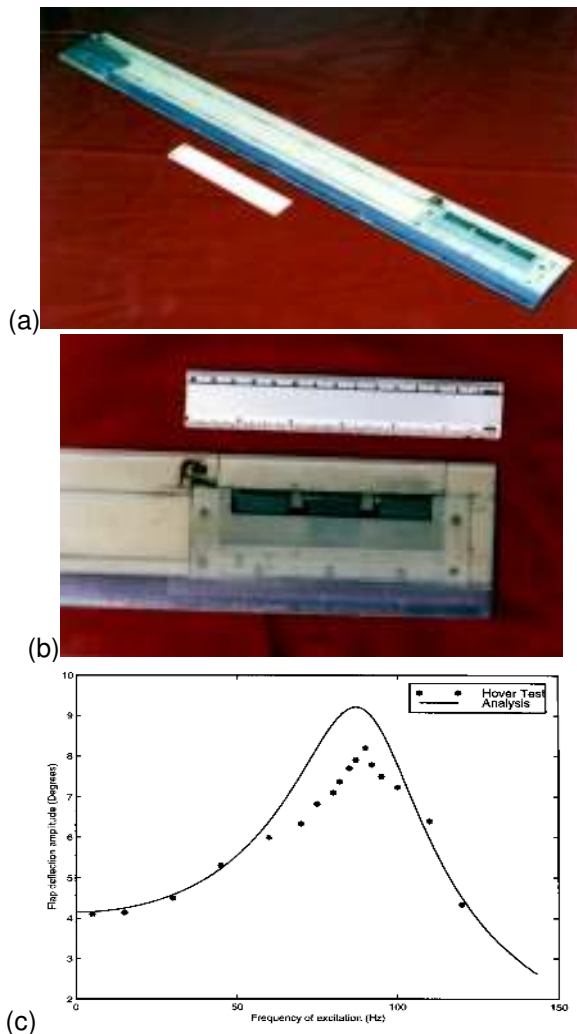


**Figure 8 (a) scaled rotor blade model with piezoelectric bimorph actuated trailing edge flap (Chopra, 1994); (b) flap details; (c) variation of flap deflection amplitude with frequency at 900 rpm in the hover test stand (Koratkarn and Chopra, 1998)**

Due to inherent limitations in the bimorph excitation concept (low mass efficiency and need for leading edge balance weights), attention was subsequently re-focused on ISA stacks (Precht and Hall, 1997).

Walz and Chopra (1994), and Koratkarn and Chopra (1998) also used bimorph ISA rotor blade flaps. Initially, Walz and Chopra (1994) used trailing edge flaps of 20% chord, 12% span ( $0.85R - 0.97R$ ) were built into a 36 in radius, 3 in chord composite blade model (Figure 8). Later, Koratkarn and Chopra (1998) used a 4% span flap actuated by a 4-layer PZT bimorph actuator.

A Hall sensor was incorporated into the blade to measure flap deflection during rotating blade testing. Testing was performed at various collective pitch values up to  $4^\circ$  collective pitch. Flap deflections of  $\pm 8^\circ$  were measured with a Hall sensor at the Froude scaled operating speed 900 rpm (Figure 8c). Fulton and Ormiston (1998) also used bimorph flap actuation.

### **C-Block and Recurved Flap Actuators**

The C-block and recurved actuators have been successfully researched at the University of Michigan by Diann Brei and her students. These actuators are similar in basic principles with the unimorph and bimorph actuators, but present certain architectural characteristics that facilitate compact arrangement in serial and parallel packs. In a joint effort between University of Michigan (Diann Brei) and University of Auburn (Ronald Barrett) these actuators were used to actuate the trailing edge flap of a wind-tunnel airfoil section.

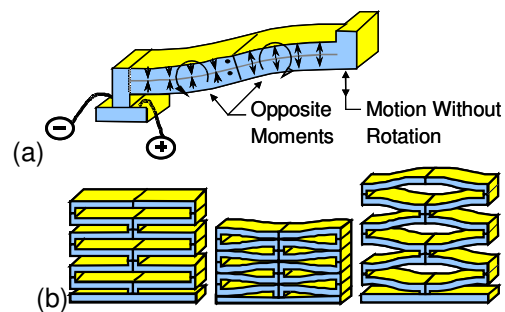


**Figure 9 Recurved actuators: (a) principle of operation; (b) series arrangements (Brei, 1999b)**

The C-block actuator (Moskalik and Brei, 1998) is fabricated from piezoceramic tubes cut in two along the generator and affixed to the either sides of an undulating metal substrate. A wind-tunnel airfoil specimen, using series and parallel C-block arrangements to achieve the necessary force and deflection (Figure 10a), was constructed (Clement

*et al.*, 1998). Wind tunnel tests yielded flap deflection of 15-25 deg peak-to-peak over a 0-40 Hz bandwidth at up to 130 ft/s flow speed (Clement and Brei, 1998; Brei, 1999a).

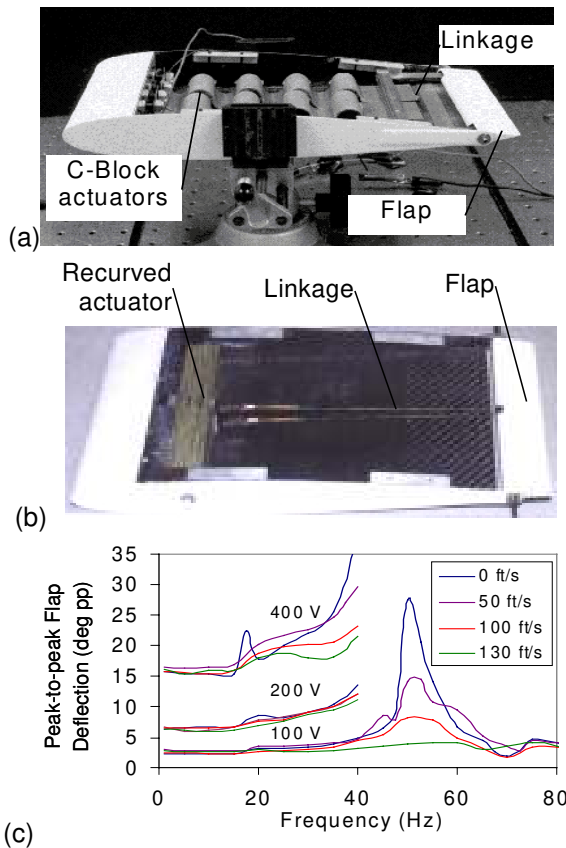


**Figure 10 Active-flap wind tunnel specimens: (a) C-block actuator variant; (b) recurved actuator variant; (c) wind tunnel test results (Brei, 1999b)**

One perceivable drawback of the C-block actuator is that the effective center of gravity of the actuator is placed well aft of the  $\frac{1}{4}$  chord axis, thus raising significant balancing and possible flutter issues. The recurved actuator offers better compactness than the C-block actuators. The recurved actuator resembles the S-shaped bimorph developed by Matey *et al.* (1987), as mentioned by Dorey and Moore (1995). The principles of the recurved actuator (Figure 9) were articulated by Ervin and Brei (1998). The series and parallel architectural options were described, and bench-top experimental results were provided.

For wind tunnel testing, a battery of recurved actuators, mounted into the forward section of the airfoil model, was used to activate the trailing edge flap. As seen in Figure 10b, the recurved actuator is much more compact than the C-block actuator and lies closer to the  $\frac{1}{4}$  chord axis. Therefore,

much less counter balance weight is expected. The wind-tunnel tests showed 15-25 deg. peak-to-peak response over the 0-40 Hz (Figure 10c).

### **Piezostacks-Actuated Active Flaps**

Precht and Hall (1996) built a mechanically amplified ISA flap actuator (X-frame actuator) using a pair of EDO Corp. EC-98 PMN-PT piezoceramic stacks with 140 layers of 0.0221-in thick = 3.1-in (~80 mm) active length. In bench tests, the actuator showed 81 mil (~2.057 mm) free displacement, for frequencies up to 200 Hz, and a blocked force of 35.8-lb (~156 N), sustained under up to 69-g 135-Hz shaking (Hall and Precht, 1999). In a 1/6 Mach scale CH-47D rotor-blade model, The X-frame actuator occupies the leading edge part of the airfoil (Figure 11).

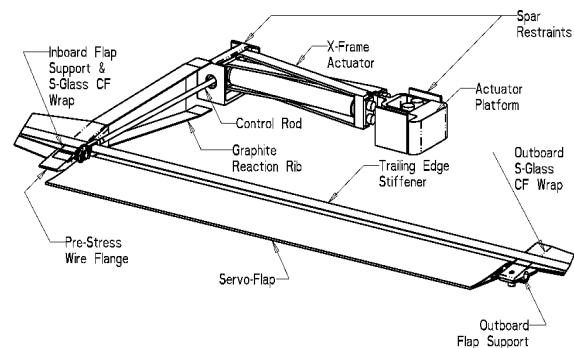


**Figure 11 The X-frame actuated servo flap (Precht and Hall, 1999)**

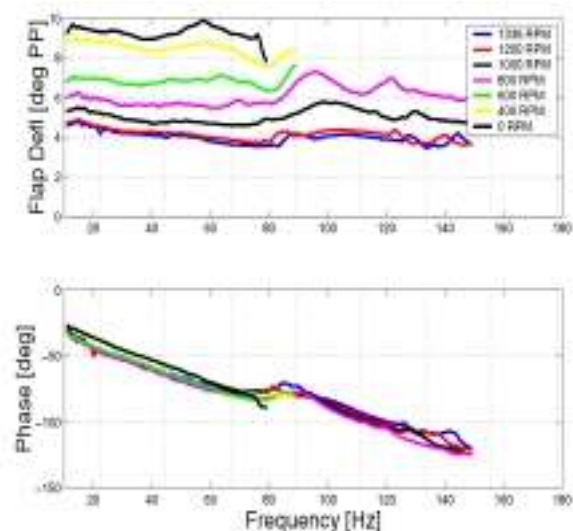


**Figure 12 Frequency response of the X-frame actuated trailing-edge flap in the 1/6 Mach scale CH-47D rotor blade model, in hover tests at various RPM's (Hall reported in Straub, 1999)**

Mechanical linkages (control rod and reaction tube) are used to actuate the trailing edge flap horn and return the reactions into the actuator structure (Prechtl and Hall, 1998). In the scaled rotor blade model, peak-to-peak deflection of almost 100 was demonstrated for frequencies up to 150 Hz (i.e., in excess of 6/rev) during bench tests (Figure 12). Hover tests performed under realistic aerodynamic loading demonstrated 4-5° over the same frequency range (Straub, 1999). Lee and Chopra (1998) also used piezostacks for servo-flap actuation of scaled rotor blade.

### **FULL-SCALE SMART ROTOR BLADE FLAP EXPERIMENTS**

A federally funded program for full-scale implementation of smart materials actuation rotor technology (SMART) is under way at Boeing Mesa, Arizona. Straub (1993) analyzed the feasibility of using active materials actuators for rotor blade control. Straub and Merkley (1995) presented a design study for the implementation of a smart rotor-blade flap on the AH-64 Apache helicopter. In a gradual approach, the full-scale proof-of-concept demonstration is initially planned on the MD 900 bearingless rotor (Straub and King, 1996). After a successful proof of concept demonstrations, future

applications on AH-64, V-22, RAH-66 and JTR are envisaged. The conceptual design calls for a trim tab for in-flight blade tracking and an active control flap for noise and vibration reduction, as shown in Figure 13 (Straub, Ealey, and Schetky, 1997).

A prototype actuator with a two-stage amplification and bi-axial operation was constructed and tested (Straub *et al.*, 1999). The actuator contained two parallel piezo-stack columns working out-of-phase in a push-pull mode. The 2-stage amplification resulted in a total stroke amplification of about 10:1. Output displacements of up to 0.4 mm were measured under simulated load conditions in a 0-40 Hz bandwidth. The stack heat transfer was studied under sustained 40-Hz operation. Temperature stabilization at +22°C (40°F) above ambient was observed, thus indicating that long-term sustained operation is feasible. The actuator was also successfully subjected to environmental qualification tests consisting of shake testing (29 g @ 2/rev) and spin testing (814 g). The total actuator weight was ~0.75 kg (1.65-lb). Presently, the SMART rotor program team consists of Boeing, Massachusetts Institute of Technology (MIT), University of California at Los Angeles (UCLA), and University of Maryland.

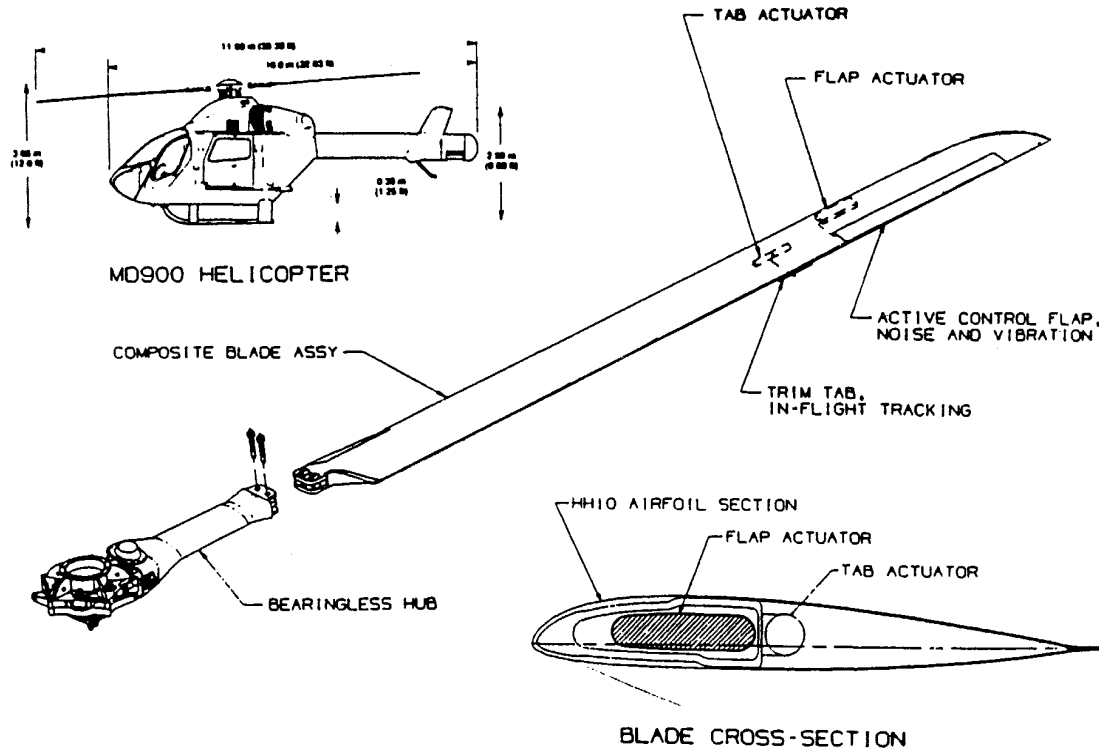


**Figure 13 MD 900 helicopter and hingeless blade displaying the planned trim tab for in-flight tracking and active control flap for noise and vibration reduction (Straub and King, 1996).**



Support to the program is also being offered by NASA Ames (40 x 80-ft wind tunnel tests), Rockwell Science Center (RSC), and TRS Ceramics, Inc.

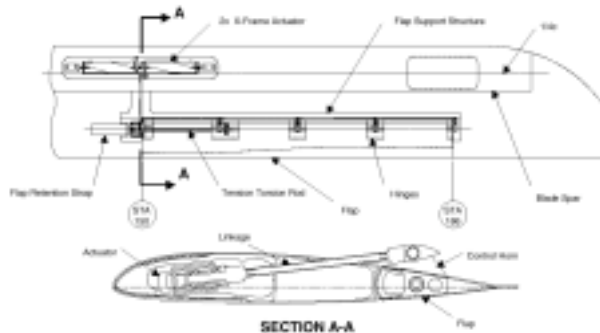


**Figure 14 Flap actuation integration for the SMART blade prototype (Straub, 1999).**

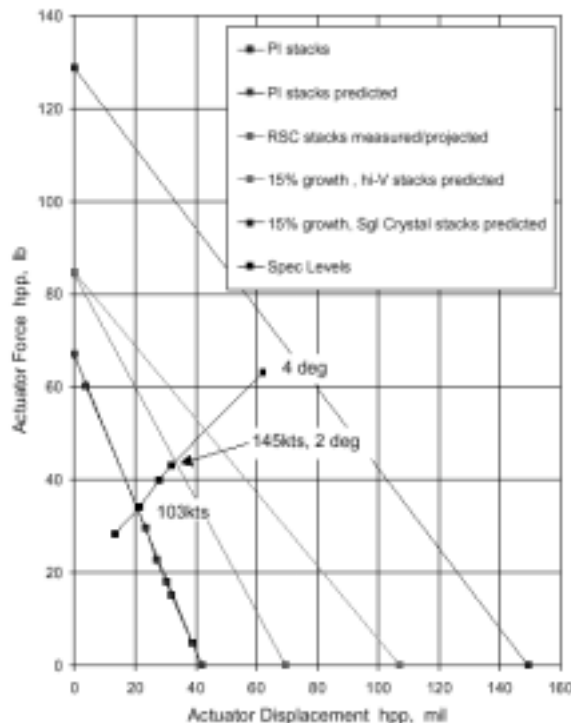


**Figure 15 Double-X actuator testing and redesign (Straub, 1999).**

A new displacement amplification principle, the double X-frame (2-X) concept has been adopted, fabricated, and tested (Figure 14). The 2-X prototype demonstrated 1-mm stroke and successfully sustained environmental and spin tests. Separate piezo-stacks selection tests conducted at UCLA identified TRS and RSC piezo-stacks with higher energy densities

(~0.555 J/kg) at optimal preload values (14 MPa). When incorporated into the 2-X actuator, such piezo-stacks are predicted to exceed the 2 deg. design specification (Straub, 1999). Up to 3 deg. flap-authority is predicted with high voltage stacks, and 40 with the novel single-crystal stacks (Figure 15).

## CONCLUSIONS

Active-materials induced-strain actuation (ISA) for aeroelastic and vibration control have evolved from laboratory scale proof-of-concept demonstrations to full-scale helicopter and airplane implementation. So far, the research efforts have channeled on two approaches: (a) distribute/continuous induced-strain actuation with embedded/distributed active materials; (b) discrete/pointwise excitation using active-material based actuators. Distributed induced-strain actuation has come at odds with the high inherent stiffness of traditionally designed structures. Consequently, experimental results, e.g., induced-strain twists, have not been very impressive. To achieve better results, a multidisciplinary optimization approach, including ISA effects, needs to be taken (Wilkie, Belvin, and Park, 1998; Schweiger, 1999; Cesnik *et al.*, 1999). Discrete actuation has been more successful, partly due to the separation of variables, and partly because it lends itself easily to retrofitting existing structures. In discrete actuation, the major challenge is to amplify the patently small active-material ISA response in order to create usable actuator stroke output. A number of ingenious solutions have been developed, especially for helicopter applications.

The advent of new induced-strain materials with very large displacement capabilities, and their imminent transition from laboratories to commercial applications, is opening new opportunities and new challenges in the field of active-materials induced-strain actuation for aeroelastic vibration control. The upcoming challenges are at system integration level. The active materials devices need to be blended into the flight-vehicle overall design requirements. The balancing of the weight and power budget at overall aircraft level is going to become the focus point of system integration. Significant power supply, airworthiness, and reliability issues are expected and will have to be overcome. Among these challenges, two seem more acute: (a) the development of compact on-board power amplifiers capable of handling the large reactive power requirement of the piezoelectric system;

and (b) the utilization of the full frequency bandwidth capability of the piezoelectric devices through frequency devolution and peak energy per cycle magnification.

### **ACKNOWLEDGEMENTS**

The authors gratefully acknowledge the financial support of the National Science Foundation through NSF/EPSCoR Cooperative Agreement No. EPS-9630167, of the US Department of Defense through South Carolina Army National Guard and the Army Research Office, and of the US Department of Energy through Sandia National Laboratories.

### **REFERENCES**

- Barrett, R. (1993) "Aeroservoelastic DAP Missile Fin Development", *Smart Materials and Structures*, Vol. 2, pp. 55-65, 1993.
- Barrett, R. and Stutts, J. (1997) "Design and Testing of a 1/12th-scale Solid State Adaptive Rotor", *Smart Materials and Structures*, Vol. 6, pp. 491-497, 1997.
- Barrett, R.; Frye, P.; Schliesman, M. (1998) "Design, Construction, and Characterization of a Flightworthy Piezoelectric Solid State Adaptive Rotor", *Smart Materials and Structures*, Vol. 7, pp. 422-431, 1998.
- Bernhard, A. P. F. and Chopra, I. (1999) "Hover Testing of Active Blade-Tips Using a Piezo-Induced Bending-Torsion Coupled Beam", *Journal of Intelligent Material Systems and Structures* (in press).
- Brei, D. (1999a) "Piezoelectric Actuators", *Technical Director's Conference: Future Challenges in Precision Munitions-Actuators and Power*, Picatinny, New Jersey, August 18-19, 1999.
- Brei, D. (1999b) "Smart Piezoelectric Actuators", *DARPA Flow Actuators Workshop*, Arlington, VA, October 25, 1999.
- Cesnik, Carlos E. S.; Shin, Sang Joon; Wilkie, W. Keats; Wilbur, Matthew L.; Mirick, Paul H. (1999) "Modeling, Design, and Testing of the NASA/ARMY/MIT Active Twist Rotor Prototype Blade", *55<sup>th</sup> Annual Forum of the American Helicopter Society*, Montreal, Canada, May 25-27, 1999.
- Cesnik, Carlos E. S.; Shin, Sang Joon (1999) "On the Twist Performance of a Multiple-Cell Active Helicopter Blade", *8<sup>th</sup> ARO Workshop on Aeroelasticity of Rotorcraft Systems*, Penn State University, October 18-20, 1999.
- Chen, P. C. and Chopra, I. (1997) "Wind Tunnel Test of a Smart Rotor Model with Individual Blade Twist Control", *SPIE* Vol. 3041, pp. 217-229.
- Chopra, I. (1994) Private communication to Professor C. A. Rogers.
- Chopra, I. (1997) "Status of Application of Smart Structures Technology to Rotorcraft Systems", *Innovation in Rotorcraft Technology*, Royal Aeronautical Society, London, UK, June 25-26, 1997.
- Clement J. W.; Brei, D.; Moskalik, A. J.; Barrett, R. (1998) "Bench-top Characterization of an Active Rotor Blade Flap System Incorporating C-block Actuators", *39<sup>th</sup> AIAA/ASME/ASCE/AHS/ASC Structures, Structural Dynamics and Materials Conference and Exhibit*, Long Beach, CA.
- Clement, J. W. and Brei, D. (1999), "Wind Tunnel Testing of a High Authority Airspeed Insensitive Rotor Blade Flap", #AIAA-99-1503, *40<sup>th</sup> AIAA/ASME/ASCE/AHS/ASC Structures, Structural Dynamics and Materials Conference and Exhibit*, St. Louis, MO.
- Dorey, A. P.; Moore, J. H. (1995) *Advances in Actuators*, Institute of Physics Publishing, 1995.
- Ervin, J.; Brei, D. (1998) "Recurve Piezoelectric Strain-Amplifying Architecture", *IEEE/ASME Transactions of Mechatronics*, Vol. 3, No. 4, pp 293-301.
- Fulton, M. and Ormiston, R. A. (1998) "Use of Piezoelectric Actuators as Elements of Intelligent Structures", *Proceedings of the 54<sup>th</sup> American Helicopter Society Forum*, Washington DC, 1998.
- Giurgiutiu, V.; Chaudhry, Z.; Rogers, C.A. (1994) "Engineering Feasibility of Induced-Strain Actuators for Rotor Blade Active Vibration Control", *Smart Structures and Materials '94*, Orlando, Florida, 13-18 February 1994 Paper # 2190-11, SPIE Volume 2190, pp. 107-122.
- Giurgiutiu, V.; Chaudhry, Z.; Rogers, C.A. (1995) "Effective Use of Induced Strain Actuators in Aeroelastic Vibration Control", *36<sup>th</sup> AIAA/ASME/ASCE/AHS/ASC Structures, Structural Dynamics, and Materials Conference and Adaptive Structures Forum*, New Orleans, LA, April 13-14, 1995, Paper # AIAA-95-1095.
- Giurgiutiu, V.; Chaudhry, Z. and Rogers, C.A. (1996) "Energy-Based Comparison of Solid-State Induced-Strain Actuators", *Journal of Intelligent Material Systems and Structures*, Vol. 7, No. 1, January 1996, Technomic Pub. Co., pp. 4-14.
- Giurgiutiu, V.; Chaudhry, Z.; Rogers, C.A. (1997a) "Design of Displacement Amplified Induced Strain Actuators for Maximum Energy Output", *ASME Journal of Mechanical Design*, Vol. 119, No. 4, December 1997, pp. 421-524.
- Giurgiutiu, V.; Craig A. Rogers, C. A (1997b) "Power and Energy Characteristics of Solid-State Induced-Strain Actuators for Static and Dynamic Applications", *Journal of Intelligent Material Systems and Structures*, Vol. 8, September 1997.
- Hall, S. R. and Prechl, E. F. (1996), "Development of a Piezoelectric Servoflap for Helicopter Rotor Control", *Journal of Smart Materials and Structures*, Vol. 5, pp. 26-34, February 1996.
- Hall, S. R. and Prechl, E. F. (1999), "Preliminary Testing of a Mach-Scaled Active Rotor Blade with a Trailing Edge Servo-Flap", *SPIE Smart Structures and Materials Symposium*, Newport Beach, CA, 1-5 March 1999, paper # 3668-03..
- Korathkar, N. A. and Chopra, I. (1998) "Analysis and Testing of a Mach Scaled Helicopter Rotor in Hover with Piezoelectric Bender Actuated Trailing-Edge Flaps", *SPIE's 1998 Symposium on Smart Structures and Materials*, San Diego, CA, March 1998, SPIE Vol. 3329, pp. 321-332, 1998.

- Matey, J. R.; Crandall, R. S.; Bryki, B. (1987) "Bimorph Driven  $x$ - $y$ - $z$  Translation Stage for Scanned Image Microscopy", *Revue Scientific Instrumentation*, Vol. 58, pp. 567-700.
- Millott, T.A.; and Friedmann, P.P. (1994) "Vibration Reduction in Hingeless Rotors in Forward Flight Using an Actively Controlled Trailing Edge Flap: Implementation and Time Domain Simulation", ", *AIAA/ASME/ASCE/AHS/ASC 35th Structures, Structural Dynamics, and Materials Conference*, Hilton Head, SC, April 18-20, 1994, #AIAA-94-1306-CP, pp. 8-22.
- Morris, D. G.; Hagood, N. W.; Pizzochero, A. (1999) "An Experimental Investigation of the Effect of Environmental Stress on Active Fiber Composite Actuators", *SPIE* Vol. 3674, pp.296-305.
- Moskalik, A. J.; Brei, Diann (1998) "Parametric Investigation of the Deflection Performance of Serial Piezoelectric C-Block Actuators", *Journal of Intelligent Material Systems and Structures*, Vol. 9, pp. 223-231, 1998.
- Narkiewicz, J. P. and Done, G. T. S. (1994) "Overview of Smart Structure Concepts for Helicopter Rotor Control", *2nd European Conference on Smart Structures and Materials*, Glasgow, U.K., 1994
- Nitzsche, F., 1993, "Modal Sensors and Actuators for Individual Blade Control", *Proceedings of the AIAA/ASME/ASCE/AHS/ASC 34th Structures, Structural Dynamics, and Materials Conference*, La Jolla, CA, April 1993, paper AIAA-93-1703-CP, pp. 3507-3516.
- Nitzsche, F., 1994, "Design Efficient Helicopter Individual Blade Controllers Using Smart Structures ", *Proceedings of the AIAA/ASME/ASCE/AHS/ASC 35th Structures, Structural Dynamics, and Materials Conference - Adaptive Structures Forum*, Hilton Head, SC, April 21-22, 1994, paper AIAA-94-1766-CP, pp.
- Prechl, E. F. and Hall, S. R. (1997), "Design of a High Efficiency Discrete Servo-Flap Actuator for Helicopter Rotor Control", *SPIE* Vol. 3041, pp. 158-182, 1997.
- Prechl, E. F. and Hall, S. R. (1998) "An X-frame Actuator Servo-Flap Actuation System for Rotor Control", *SPIE* Vol. 3329, pp. 309-319, 1998.
- Rodgers, J. P. and Hagood, N. W. (1998) "Preliminary Mach-Scale Hover Testing of an Integrated Twist-Actuated Rotor Blade", *SPIE* Vol. 3329, pp. 291-308, 1998.
- Schweiger, Johannes; Simpson, John; Weiss, Franz; Coetzee, Etienne; Boller, Christian (1999) "Needs for the Analysis and Integrated Design Optimization of Active and Passive Structures for Active Aeroelastic Wings", *SPIE 6th Smart Structures and Materials Symposium*, Newport Beach, CA, March 1999, *SPIE* Vol. 3668, pp. 117-130.
- Spangler, R. L. Jr.; and Hall, S.R. (1989) "Piezoelectric Actuators for Helicopter Rotor Control", *Report # SSL 1-89, SERC 14-90*, MIT Space Engineering Research Center, Massachusetts Institute of Technology, Cambridge, Massachusetts 02139, Jan., 1989.
- Straub, F. K. (1993) "A Feasibility Study of Using Smart Materials for Rotor Control", *49th Annual Forum of the American Helicopter Society*, St. Louis, MO, May 19-21, 1993.
- Straub, F. K. and Merkley, D. J. (1995) "Design of a Smart Material Actuator for Rotor Control", *SPIE Smart Structures and Materials Symposium*, San Diego, CA, February 26 – March 3, 1995.
- Straub, F. K.; King, R. J. (1996) "Application of Smart Materials to Control of a Helicopter Rotor", *SPIE Symposium on Smart Structures and Materials*, San Diego, CA, February 26-29, 1996.
- Straub, F. K.; Ealey, M. A.; and Schetky, Mac L. McD. (1997) "Application of Smart Materials to Helicopter Rotor Active Control", *SPIE* Vol. 3044, pp. 99-113, 1997.
- Straub, F. K.; Ngo, H. T.; Anand, V.; Domzalski, D. B. (1999) "Development of a Piezoelectric Actuator for Trailing Edge Flap Control of Rotor Blades", *SPIE Symposium on Smart Structures and Materials*, Newport Beach, CA, March 1-4, 1999, *SPIE* Vol. 3688, Part One, pp. 2-13.
- Straub, F. K. (1999) "Development of a Full Scale Smart Rotor System", *8th ARO Workshop on Aeroelasticity of Rotorcraft Systems*, Penn State University, October 18-20, 1999.
- Walz, C., and Chopra, I., 1994, "Design, Fabrication, and Testing of a Helicopter Rotor Model with Smart Trailing Edge Flaps", *AIAA/ASME/ASCE/AHS/ASC 35th Structures, Structural Dynamics, and Materials Conference - Adaptive Structures Forum*, Hilton Head, SC, April 21-22, 1994, paper AIAA-94-1767-CP, pp. 298-319.
- Wilbur, Mathew L.; Wilkie, W. Keats; Yeager, Jr., William T.; Lake, Renee C.; Langston, W; Cesnik, Carlos E. S.; Shin, Sang Joon (1999) "Hover Testing of a NASA/ARL/MIT Active Twist Rotor", *8th ARO Workshop on Aeroelasticity of Rotorcraft Systems*, Penn State University, October 18-20, 1999.
- Wilkie, W. K.; Belvin, W. K.; and Park, K. C. (1998) "Torsional Stiffness Optimization of Piezoelectric Active Twist Helicopter Rotor Blades", *9th International Congress on Adaptive Structures and Technologies*, October 14-16, 1998, Boston, MA, pp. 213-224.
- Wilkie, W. Keats; Wilbur, Matthew L.; Mirick, Paul H. Cesnik, Carlos E. S.; Shin, Sang Joon; (1999) "Aeroelastic Analysis of the NASA/ARMY/MIT Active Twist Rotor", *55th Annual Forum of the American Helicopter Society*, Montreal, Canada, May 25-27, 1999.